Relating grass failure on the landside slope to wave overtopping induced excess normal stresses

Ponsioen, Luc; van Damme, Myron; Hofland, Bas; Peeters, Patrik

DOI
10.1016/j.coastaleng.2018.12.009

Publication date
2019

Document Version
Accepted author manuscript

Published in
Coastal Engineering

Citation (APA)
Ponsioen, L., van Damme, M., Hofland, B., & Peeters, P. (2019). Relating grass failure on the landside slope to wave overtopping induced excess normal stresses. *Coastal Engineering*, *148*, 49-56. https://doi.org/10.1016/j.coastaleng.2018.12.009

Relating grass failure on the landside slope to wave overtopping induced excess normal stresses

Luc Ponsioen

Aveco de Bondt, Podium 9, 3800 GE Amersfoort, The Netherlands

Myron van Damme

Delft University of Technology, Department of Hydraulic Engineering, Stevinweg 1, 2600 GA Delft, The Netherlands

Bas Hofland

Delft University of Technology, Department of Hydraulic Engineering, Stevinweg 1, 2600 GA Delft, The Netherlands

Patrik Peeters

Flanders Hydraulics Research, Flemish Authorities, Berchemlei 115, 2140 Antwerpen Borgerhout, Belgium

Abstract

A high quality safety assessment of levee systems requires a good prediction of when the grass cover of levees fail. Current methods relate the onset of failure to the peak in momentum or energy of the flow, instead of the peak in momentum transfer or energy transfer to the grass cover. The critical velocity necessary in the current methods is thereby difficult to quantify. In line with determining the peak in momentum transfer to the grass, here is shown that the onset of damage of the grass cover can be related to the peak normal stresses acting on the grass cover during wave overtopping. The peak in momentum transfer is thereby assumed to be located at the point of reattachment of the flow with the landside slope. The method is validated against the results of two wave overtopping experiments and benchmarked against the cumulative overload method. An advantage of this method is thereby that both the time and location of the onset of damage can be predicted.

Keywords: Wave Overtopping, Wave Impact Method, Cumulative Overload Method, Grass Failure, Levee

1. Introduction

In line with the new risk based safety assessments performed on levees in The Netherlands and Belgium, the probability of levee failure with respect to applied loads needs to be assessed. An important failure mechanism is erosion of the landside slopes by overtopping waves, as indicated by the 1953 flood of The Netherlands or the effects of Hurricane Katrina in 2004. The most common cover layer of these landside slopes consists of grass on clay. To evaluate the erosion resistance of grass covers on the landside slope of levees, multiple large scale wave overtopping experiments have been performed (Van der Meer et al., 2012). Based on these tests empirical approaches have been developed that relate the damage to grass covers to the local flow velocity, shear stress, or stream power (Dean et al., 2010; Hughes, 2011; Van der Meer et al., 2012).

In this paper, first the main characteristics of the existing empirical approached for predicting grass failure on landside slopes are discussed. Next, the inferred damage mechanism and the approach for evaluating the impact of the momentum transfer by normal stresses is presented in Section 2. In Section 3, the approach is validated against two field scale wave overtopping experiments. The results are evaluated in Section 4, and conclusions and recommendations are presented in Section 5.

1.1. Damage formation to grass

1.1.1. Existing approaches

Up to a decade ago damage to grass slopes on the landside slopes of levees was mostly related to the mean overtopping discharge (Van der Meer, 2002). Lately, more local hydraulic loads are used to empirically quantify the erosion resistance of grass covers subject to overtopping waves. Dean et al. (2010) used the critical velocity concept for steady overflow from CIRIA 116 (Hewlett, 1985),(Whitehead et al., 1976) to arrive at a relationship for the failure of levees due to overtopping. Dean et al. (2010) thereby related the damage initiation of grass to a mean excess velocity, excess shear stress, or excess stream power. The excess stream power showed the smallest errors and was therefore the recommended method of damage description. Van der Meer et al. (2012) extended the approach by Dean et al. (2010). Instead of using mean values for the shear stress or stream power, Van der Meer et al. (2012) hypothesized that peak loads during wave overtopping are likely to contribute significantly more to the onset of damage than mean loads. This led to the cumulative overload method. For a certain location on the grass cover, the cumulative overload method predicts a damage factor D from (Van der Meer et al., 2012).

$$D_{\mathrm{CO}} = \sum_{i=1}^{i=n} \left(a_p u_p^2 - u_c^2 \right) \tag{1}$$

where u_c is the critical velocity [m/s] and u_p is the peak velocity [m/s] that follows empirically from (Van der Meer et al., 2012):

$$u_p = 4.5V^{0.3} \tag{2}$$

With V the wave overtopping volume [m^2] and a_p is a flow acceleration factor which will be larger than 1, increasing down the slope. According to Van der Meer et al. (2012) initial damage is expected when D_{CO} = 500, severe damage should be observed when D_{CO} = 1000 and complete failure occurs when D_{CO} = 3500. These values are prone to large scatter.

Characteristic of these approaches (Dean et al., 2010; Hughes, 2011; Van der Meer et al., 2012) is that damage is assumed to initiate when a velocity, shear stress, or stream power exceeds a critical value. The summation of the excess load is an indicator of the extent of the damage induced by overtopping waves. The cumulative overload method by Van der Meer et al. (2012) is stress based and consequently related to u^2, whereas the mean excess load approach (Dean et al., 2010; Hughes, 2011) is energy based and uses u^3. As the flow velocity increases along the landside slope, due to acceleration of the flow by gravity, damage is consequently most likely to initiate at the toe of the landside slope.

A close evaluation of the excess velocity, stress, or stream power (Dean et al., 2010; Hughes, 2011) or cumulative overload (Van der Meer et al., 2012) have highlighted two problems. First, critical velocity values required for these methods are difficult to quantify. During steady overflow tests performed on grass (van Damme et al., 2016; Cantré et al., 2017) it was noted that the critical velocity needed to initiate damage to the grass far exceed predictions given by Hewlett (1985) and Whitehead et al. (1976). Second, according to the excess stress or excess volume approach grass covers should predominantly fail near the bottom of the landside slope as the energy of the flow is maximum there due to the acceleration of the flow along the landside slope. However grass has also been observed to fail near the top of the landside slope. Below the second knowledge gap is addressed, whether damage initiation should be correlated only with the slope parallel flow velocity, or (also) with the peak in momentum transfer perpendicular to the levee. This is done by relating damage to the normal stresses exerted on the grass by overtopping waves.

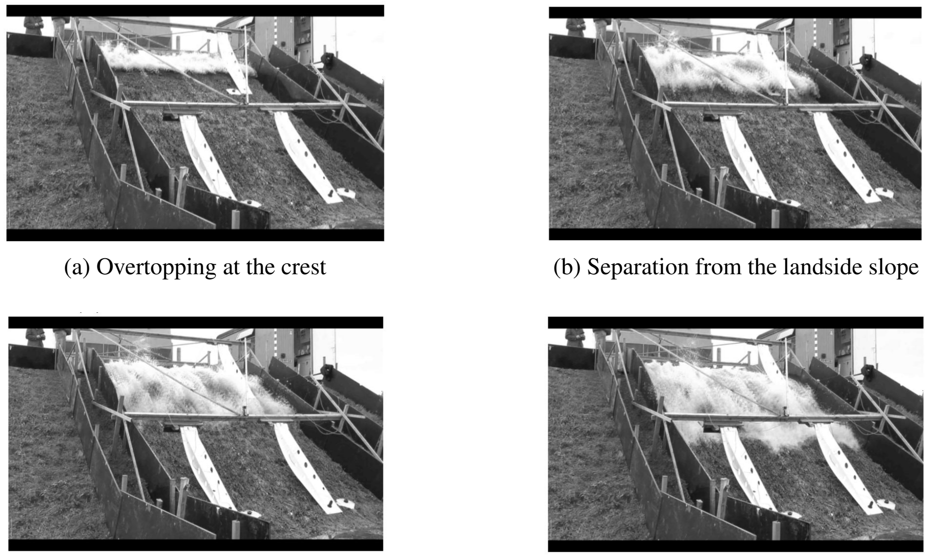

(a) Overtopping at the crest

(b) Separation from the landside slope

(c) Close to reattachment with landside slope

(d) Point of impact

Figure 1: Wave separation from the bed and an impact during a 2 m^3/m overtopping wave volume. Observed during wave overtopping tests at Wijmeers, Belgium.

1.1.2. Proposed approach

During wave overtopping experiments performed at Wijmeers (van Damme et al., 2016) it was noted that overtopping waves separated at the end of the crest before reattaching with the landside slope, as can be seen in Figure 1. The impact of an overtopping wave was more powerful and the impact zone was further down the landside slope than the impact of overtopping flow due to a higher flow velocity at the crest. It was inferred that at the point of reattachment both shear stresses and normal stresses are transferred to the levee surface. The significant normal stress component at the point of reattachment of overtopping waves causes for a peak in momentum transfer higher up the landside slope. Differences in normal stresses exerted on the landside slope of the levee between overflow and overtopping would explain why grass covers fail during overtopping but not during overflow. Here the hypothesis is tested whether the location of damage on the landside slope due to wave overtopping could be caused by peaks in momentum transfer due to the normal impact by overtopping waves.

The envisaged damage mechanism by which the grass cover fails is depicted in Figure 2. Grass failure is expected to start with existing small cracks in the grass/clay cover (See Figure 2a). These cracks are often present due to natural expansion

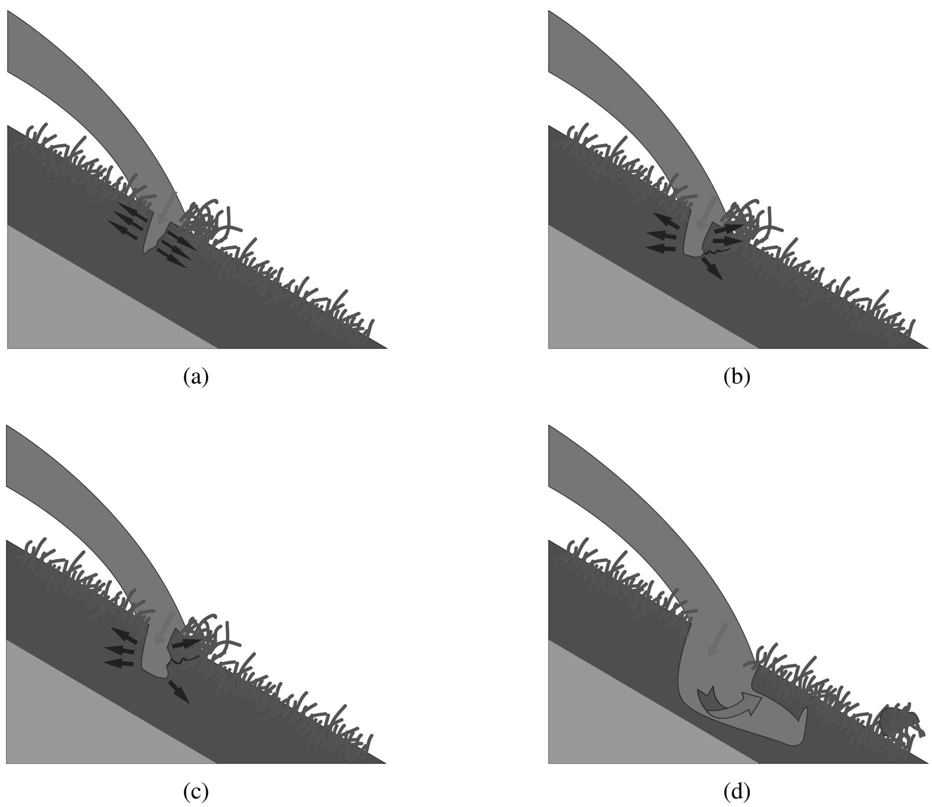

Figure 2: Failure initiation process observed during the overtopping experiment at Wijmeers

and shrinkage of the clay cover. Normal forces exerted on the landside slope by overtopping waves (Figure 2b) cause these cracks to widen. In accordance with Führböter (1966), the increase in water pressure in the crack during wave impact is expected to push the walls of the crack aside and cause for the crack to deepen. When the crack extends over the depth of the turf layer, grass can reasonably be expected to become subject to deformation due to lower cohesion of the clay under the turf layer compared to that of the root/clay mixture (Figure 2c). The hole that originates under the grass cover will then cause for the grass aggregate to be pushed up (Figure 2d), allowing for further expansion of the hole under the grass by flow induced scour. The continuous increase of space beneath the grass, causes grass aggregates to be pushed out of the soil. The flow over the grass cover and the overpressure under the grass cover separates the grass sod from the clay layer, making it roll up like a carpet in downstream direction, which is in accordance with observations made by Hai and Verhagen (2014). At a certain moment the induced pressure under the grass cover becomes too high leading to a piece of grass sod to be ripped from the grass cover and washed away by the flow.

Depending on the curvature of the levee at the intersection of the crest and landside slope overtopping waves separate from the landside slope at the downstream end of the crest before reattaching with the landside slope further down the landside slope (see Figure 1). The point of reattachment of large volume waves is thereby located further downstream than for small volume waves. This is due to the higher horizontal flow velocity component at the downstream end of the crest. This process was observed during the Wijmeers overtopping experiments (van Damme et al., 2016) whereby immediate failure of the grass cover initiated after one 3000 l per m wave. The hypothesis that the location of grass failure is related to the summation of normal stresses exerted by overtopping waves to the slope at the location of reattachment is furthermore supported by reports on the overtopping experiments in Zeeland (Bakker et al., 2008). Here damage to the grass cover first initiated at the end of the landside slope where the flow was redirected and hence a significant momentum was exchanged with the grass cover. Based on this hypothesis a new approach was developed which relates the initiation of damage to the normal stresses at the point of reattachment. Hereonwards this approach is referred to as the wave impact approach.

2. Wave impact approach

2.1. Normal stresses acting on the grass cover

To evaluate the normal stresses exerted on the levee the location of wave impact is determined and compared to the location of the (initial) damage. In a Cartesian reference framework, the horizontal distance traveled by a wave is given by

$X(t) = u_x(t) \cdot t$, where $X(t)$ is the horizontal, time dependent, coordinate of reattachment relative to the intersection of the crest and landside slope, $u_x(t)$ is the horizontal velocity component, t [s] is the separation time. During the separation time, the wave is curved downwards under influence of gravity. The vertical distance travelled is thereby given by $Z(t) = -\frac{1}{2}gt^2$, where $Z(t)$ is the relative vertical distance travelled, and g is the gravitational constant.

Here the flow characteristics are obtained from the following approximation provided by Hughes et al. (2012). The peak discharge q_p [m^2/s] at the end of the crest has been related to the overtopping wave volume V [m^2] via (Hughes et al., 2012)

$$q_p = 0.184\sqrt{g}V^{\frac{3}{4}} \tag{3}$$

T_0 is the overtopping duration which can be derived from the wave volume according to (Hughes et al., 2012) (with dimensions for q_p, V, and T_0, respectively m^2/s, m^2, and s).

$$T_0 = \frac{V^{1.16}}{0.43q_p} \tag{4}$$

Under the assumption that d_p and u_p appear at the same location (Hughes, 2011), the reduction in depth and velocity over time are given by

$$u_{\text{crest}}(t) = u_p\left(1 - \frac{t}{T_0}\right)^a \tag{5}$$

$$d_{\text{crest}}(t) = d_p\left(1 - \frac{t}{T_0}\right)^b \tag{6}$$

Here a and b are parameters which determine the matter of decrease in velocity or water depth with time. Often this decrease is assumed to be linear, therefore both a and b are assumed to be 1. The peak depth d_p [m] could be related to the peak discharge according to (Hughes et al., 2012)

$$q_p = \left(\frac{2}{3}\right)^{\frac{3}{2}}\sqrt{g}\,d_p^{\frac{3}{2}} \tag{7}$$

Assuming d_p and u_p appear at the same location, the peak velocity u_p is determined by

$$u_p = \frac{q_p}{d_p} \tag{8}$$

Assuming a uniform velocity distribution over the water depth at the downstream side of the crest, the extents of the wave impact area per unit width have now been determined by a new approach named the Wave Impact approach. The area of impact is thereby assumed to equal the flow area at the end of the landside slope. Any errors in mass balance have thereby been assumed negligible. The extents of the impact zone are defined by $X_{\text{wave,min}}(t)$, $Z_{\text{wave,min}}(t)$ and $X_{\text{wave,max}}(t)$, $Z_{\text{wave,max}}(t)$. The horizontal velocity component at the location of impact is assumed to be identical to the horizontal velocity component at the downstream end of the crest (see Equation 5) which leads to

$$Z_{\text{wave,min}}(t) = -\frac{1}{2}g\left(\frac{X_{\text{wave,min}}(t)}{u_{\text{crest}}(t)}\right)^2 = -X_{\text{wave,min}}(t)\tan\theta \tag{9}$$

where θ is the slope angle of the landside slope, and

$$X_{\text{wave,min}}(t) = \frac{2 \cdot u^2_{\text{crest}}(t)\tan\theta}{g} \tag{10}$$

Equations 9 and 10 could be written for the maximum impact coordinates by replacing $X_{\text{wave,min}}(t)$ and $Z_{\text{wave,min}}(t)$ for $X_{\text{wave,max}}(t)$ and $Z_{\text{wave,max}}(t)$. The vertical velocity component at the point of impact follows from

$$u_z(t) = \sqrt{2gZ_{\text{wave}}(t)} \tag{11}$$

The maximum location of impact is defined in a similar way as the minimum impact coordinate, with addition of the flow depth at the crest. The maximum impact coordinate is assumed to be determined by the top of the stream at the crest. When the streamline of the top of the flow is tracked, the maximum impact location is found. When d_{crest} is the flow depth at the crest, the maximum impact location is determined by

$$X_{\text{wave,max}}(t) = \frac{u^2_{\text{crest}}(t)}{g}\left(\tan\theta + \sqrt{\tan^2\theta + \frac{2gd_{\text{crest}}(t)}{u^2_{\text{crest}}(t)}}\right) \tag{12}$$

whereby u_{crest} and d_{crest} are obtained from Equations 5 and 6. With u_x and u_z known in the Cartesian coordinate system, the velocities can also be obtained in the $\hat{\chi}, \hat{\zeta}$ coordinate system whereby the $\hat{\chi}$ coordinate direction is parallel to the landside slope and the $\hat{\zeta}$ coordinate direction is perpendicular to the landside slope. θ is the angle with which the coordinate system rotates which is here equal to the landside slope angle. When the angle of impact of the overtopping wave on the landside slope is determined by β, the stress delivered to the landside slope due to the normal impact is now given by

$$\sigma_{\zeta\zeta} = \rho u_\zeta |u_{imp}| \sin\beta = \rho\left(u\sin\theta + \omega\cos\theta\right)\sqrt{u^2+\omega^2}\sin\beta \tag{13}$$

where u_{imp} is the impact velocity. The wave impact induces a pressure on the grass cover which is assumed to be related to the location and initiation of failure of the grass cover. It should be noted that Equation 13 describes the pressure which is exerted on a slope under steady state flow conditions. The actual normal force at the initial impulsive impact may be different. However, for a first assessment of the validity of the wave impact approach the steady state pressure approximation was deemed sufficient. This is demonstrated in Figure 3.

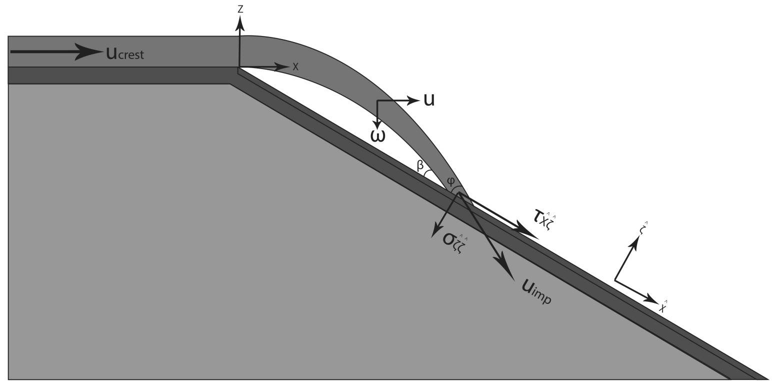

Figure 3: Normal stress per unit width approach

During an overtopping event the discharge, depth, and flow velocity of a wave decrease. The location of impact thereby retreats along the landside slope towards the crest. This phenomenon is demonstrated in Figure 4. The location and initi-

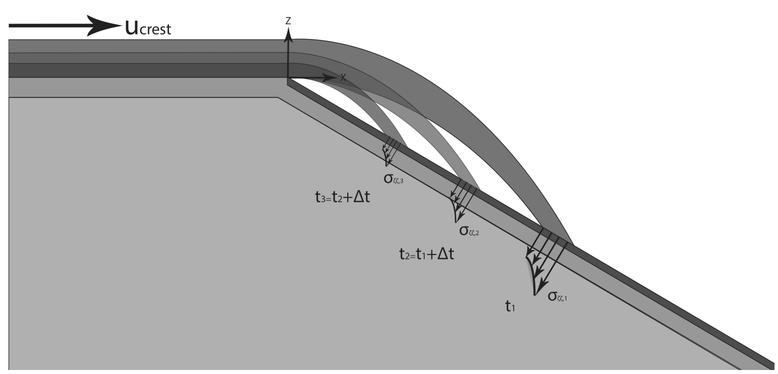

Figure 4: Changes in impact location during a single overtopping event

ation of grass failure are assumed to be related to the total transfer of momentum J_ζ which is given by the normal stress multiplied by duration. During a single wave overtopping event the area of wave impact is retreating in upstream direction. Hence, per overtopping event the net area affected by one wave is larger than the initial area of impact but encompasses the area upstream of the initial impact area. A small normal stress applied for a longer time thereby can produce a similar transfer of momentum (the same impulse) as a large stress applied briefly. Hence the location of damage initiation does not have to coincide with the area of impact of the largest waves. Supplementary to this phenomenon, the top of the wave reattaches slightly further down the landside slope than the bottom of the wave. As the overtopping discharge and velocity decrease, the top of the wave retreats over the initial points of impact on the slope of the bottom of the wave.

To determine the exchange of momentum to a specific location on the landside slope, each overtopping induced stress event at location X is integrated over time. When multiple waves overtop the levee and reattach on the landside slope, the total transferred momentum at location X is determined by the summation of the integrals of all overtopping waves. This is given by

$$J_\zeta(X) = \sum_{n=1}^{N} \int_t^T \sigma_{\zeta\zeta,n}(X,t)dt \tag{14}$$

where $\sigma_{\zeta\zeta,n}$ is a function of location X and time t. N is the amount of overtopping wave events and T is the duration over which the momentum is transferred at location X. $\sigma_{\zeta\zeta,n}(X,t)$ in Equation 14 is written in terms of horizontal land side slope coordinate $X(t)$ and flow velocity at the crest u_{crest} according to

$$\sigma_{\zeta\zeta}(t) = \rho(u^2_{\text{crest}}(t) + 2gX(t)\tan\theta)\cdot\sin\beta \tag{15}$$

For $X(t)$ see Equation 12. Damage initiates when the stresses induced on the landside slope exceeds a critical pressure. In order to evaluate whether the forces acting on the grass cover are significant to initiate damage, the resistance of the grass cover has been evaluated below.

2.2. *Resistance of the grass cover to normal stresses*

Stanczak (2007, 2008) and Führböter (1966) hypothesized for plunging waves connecting with a grass cover on the waterside slope that the wave impact pressure induces two horizontal forces. Based on an undrained failure of clay Stanczak (2007, 2008) and Führböter (1966) stated that a crack forms or widens when the impact pressure exceeds the threshold pressure P_c denoted by twice the cohesion of the clay layer. Richwien (2003) extended the approach of Führböter (1966) by including other parameters such as the weight of the soil body G, the reaction of the soil Q and the pore water pressure U based on a simplified, graphical analysis of forces. Stanczak (Stanczak, 2008, 2007), criticized the theories developed by Führböter (1966) and Richwien (2003) as they assume an idealized situation. Stanczak however did also admit that application of more advanced models is challenging. Here the theory developed for the impact of plunging waves on waterside slopes by Führböter (1966) has been applied to the case of overtopping waves impacting on the landside slope. The threshold pressure P_c, required to enlarge cracks in the grass cover, is given by the strength of clay and grass combined. Figure 2 demonstrates how pressures in excess of the critical pressure cause the walls of a crack to be pushed aside. The critical pressure of twice the cohesion (Führböter, 1966) corresponds well with the theoretical threshold stress level of cutting clay underwater as done during dredging (Miedema, 2014). However cutting tests performed with steel blades on clay indicate that the critical pressure P_c is a function of several factors like the geometry and loading situation. In general the critical pressure level is expected to vary between $2c' \leq P_c \leq 5c'$ (Van der Schrieck, 2006). A value of $5c'$ also corresponds with the artificial root cohesion found by Hoffmans (2014). It should thereby be noted that the effects of artificial cohesion by capillary action are not accounted for. The characteristic value of c' is therefore likely to be conservative. However the value may correspond with the degree of cohesion of weaker spots on the landside slope. In the remained of this paper has been assumed that the critical pressure required to initiate damage is given by $2c' \leq P_c \leq 5c'$. Damage to the grass cover is initiated when the wave impact induced normal stress delivered to the landside slope $\sigma_{\zeta\zeta}$ exceeds the critical pressure P_c.

The location of failure is assumed to coincide with the location where the total excess momentum transferred J_E is maximum. This location now follows from

$$J_E = \sum_{n=1}^{N} \int_{t}^{T} (\sigma_{\zeta\zeta,n}(X,t) - P_c) dt \tag{16}$$

Equation 16 highlights the main benefit of the wave-impact approach over the excess volume approach, namely that it is possible to validate the wave impact approach based on the location of failure, as well as the moment of initiating failure. Below, the wave impact approach has been tested and bench-marked against the excess volume approach of Van der Meer et al. (2012).

3. Testing of the wave impact approach

The assumption that the failure of grass is related to the sum of normal stresses exerted on a slope during wave overtopping has been tested against the results of two wave overtopping experiments. The first experiment was the experiment performed at Wijmeers (van Damme et al., 2016) and the second was the overtopping experiments performed in Zeeland (Bakker et al., 2008). For those overtopping tests where damage on the landside slope occurred a value for the critical stress P_c was determined based on prior performed overtopping tests on the same test section at a lower mean overtopping discharge. After setting the value for P_c the results were compared against the location of damage that was observed during the wave overtopping tests to evaluate how well the peak momentum transferred coincided with the location of initial damage on the landside slope. The found value of P_c was then compared with the theoretical value.

For the Wijmeers experiment, the wave overtopping volumes that had been released on the levee were obtained from the testing script. For the experiments in Zeeland, the exact overtopping volumes were recreated assuming Weibull distributed wave overtopping volumes. The shape and scale parameters for the Weibull distribution were obtained from the test description and the EurOtop manual (EurOtop, 2007). Based on the overtopping volumes the peak discharge was derived from Equation 3. The peak depth and peak velocity at the end of the crest were derived from respectively Equations 7 and 8, and the overtopping time was obtained from Equation 4. The velocity at the end of the crest was assumed to reduce linearly with time (see Equation 15) and uniformly distributed over the depth. The depth was divided in 10 equal sized slices. For each time step of 0.01 s the location of impact and corresponding normal stress has been assessed. The landside slope has been subdivided into a grid of 0.10 m wide. The momentum transferred in each grid cell has been added up to arrive at a distribution of total momentum transfer along the landside slope.

3.1. Wijmeers

During the Wijmeers experiment two dike sections were subjected to wave overtopping tests and 2 sections to overflow tests. During the overflow tests it became apparent that the grass cover was able to withstand mean overflow discharges of 170 l/s per m whereby the flow velocities were in excess of 3.5 m/s (van Damme et al., 2016). During the overtopping tests the first 4 m wide test section was subjected to wave overtopping volumes of respectively 1, 5, 10, 25 l/s and 50 l/s per m. The second 4 m wide test section was subjected to waves of 25 l/s per m after the hydraulic measurements had been performed on this section. A full test description is provided by (van Damme et al., 2016). The wave conditions underlying the test programme are provided in Table 1. In Table 1 V_p denotes the maximum overtopping volume, N_{ot} the number of overtopping waves, P_{ot} the overtopping probability, T_p $[s]$ the peak wave period, H_s the significant wave height, and q the mean overtopping discharge.

During the first overtopping experiment the crest line was located 3 m from the outflow opening of the simulator. Along the slope at a distance of approximately 1 m the surface of the slope had clearly dropped, however the grass cover was still intact. The corresponding critical stress for the grass cover at Wijmeers was therefore calibrated at $P_c = 10$ kN/m^2, which corresponds with a situation whereby no

Table 1: Overtopping parameters Wijmeers.

q $[l/s/m]$	1	5	10	25	50
H_s $[m]$	0.4	0.6	0.8	1.2	1.3
T_p $[s]$	2.53	3.10	3.58	4.38	4.56
P_{ot}	0.181	0.336	0.386	0.449	0.575
N_{ot}	617	936	931	858	1089
V_p $[l/m]$	113	349	672	1662	2230

damage at all would occur to the grass cover during a 5 l/s per m test. It should however be noted that at a distance of 1m along the landside slope already some settlement occurred during the 5 l/s per m test. However this settlement was initiated by a locally present rabbit hole and was not believed to be due to the forces exposed on the grass cover by the overtopping waves. A damage occurring around the 1 m line corresponds with a horizontal distance of $X = 0.85m$. Applying this critical stress value to Equation 16 gives the distribution of transferred momentum along the Cartesian x-axis shown in the top graph in Figure 5. As the second test section was located close to the first test section, the same value for the critical pressure was applied. On this second test section first hydraulic measurements were performed with wave volumes of 500 l/m increasing incrementally at steps of 500 l/m to waves of 3500 l/m. With the exception of the 3000 and 3500 l/m waves every wave volume had been released three times in concession. The larger waves already damaged the top layer of the grass cover although the root system was still in place. The damage was predominantly focused on the lower half of the landside slope. During the 25 l/s per m test, damage progressed predominantly at a horizontal distance of $1.3 \leq X \leq 2.15$ m from the landside end of the crest. The distribution of momentum exchange for this experiment is given in Figure 5b.

In Figure 5b 2 lines have been presented. The line with $P_c = 10$ kN/m^2 is based on the assumption that no damage is allowed to occur for the 1 and 5 l/s per m experiments. The second line is calibrated against the observed location of damage during Experiment 1. During the first overtopping experiment the grass cover failed at the location of a rabbit hole just beneath the surface. For a slightly sandy clay subsoil the estimated value of cohesion c' is 5 kN/m^2. The more sand is present the lower the expected value of the cohesion is. The value of P_c whereby damage initiates therefore corresponds with a value of $P_c = 2c'$.

For comparison the cumulative overload method has been applied to the results of the Wijmeers experiment in eq.(2). Figure 5c shows the damage factor as a function of the critical velocity for each of the tests performed at Wijmeers. The damage factor for severe damage (D = 1000) is represented in 5c with a horizontal

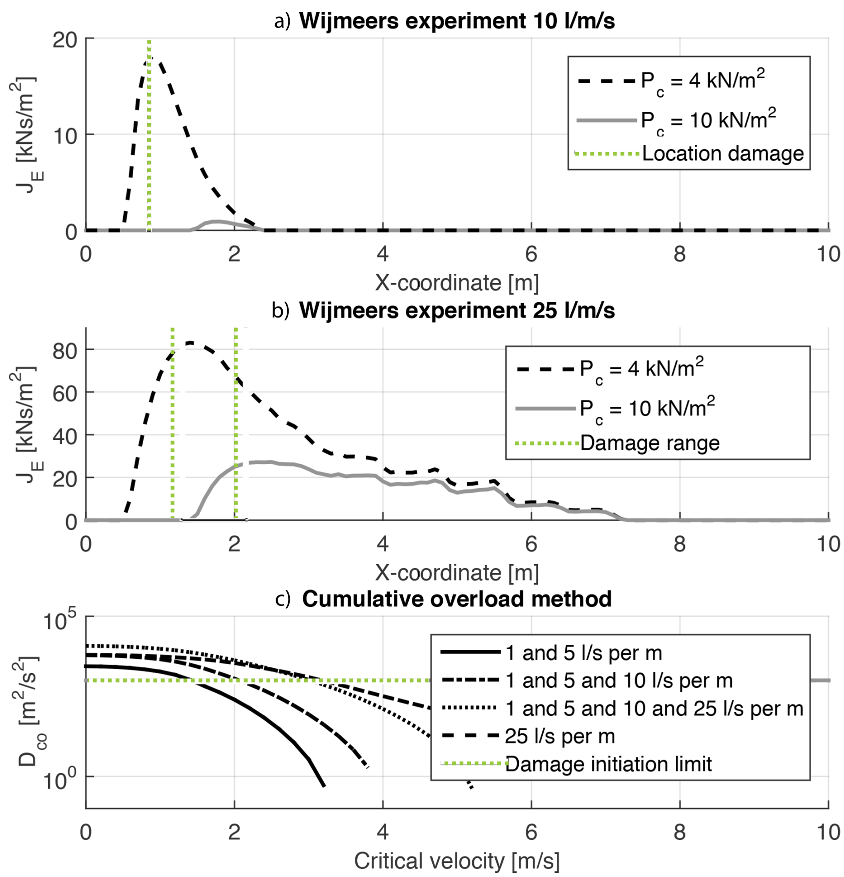

Figure 5: Distributions of excess momentum transferred to the landside slope during the overtopping experiments at Wijmeers (figure a and b), two curves are presented; a) dotted line with $P_c = 4\ \mathrm{kN/m^2}$ refers to the rabbit hole and b) $P_c = 10\ \mathrm{kN/m^2}$ refers to the highest critical pressure at which damage could be expected. The results of the cumulative overload method when applied to Wijmeers are presented in figure c.

line. At Wijmeers damage started during the 10 l/s per m overtopping test and significantly grew during the 25 l/s per m overtopping experiment. This corresponds with a critical velocity value of 2 m/s, which in turn corresponds with the critical velocity that follows from the grass resistance curves given in the Technical Note 71 (Whitehead et al., 1976). However during overflow tests, it was noted that grass was able to withstand flow velocities in excess of 3.5 m/s. This difference in critical velocity may highlight that the methods by Hughes (2011), Dean et al. (2010) and Van der Meer et al. (2012) might need some modification as the Wijmeers experiments indicate that the theoretical critical velocities do not well match the observed critical velocities.

3.2. St. Philipsland overtopping experiments

The tested landside slope at the St. Philipsland dike was 13 m long with a $1 : 2.4$ slope, or a slope angle $\theta = 0.39$ rad. The grass cover was in good conditions according to the VTV2006 standards. Below the grass cover a clay layer of approximately 0.40m thickness was present. For a good quality clean clay the expected undrained cohesion values are according to Table 2b of the NEN 1997: $c' = 13 - 15\text{kN/m}^2$. The wave overtopping conditions to which the levee was exposed are given in Table 2

Table 2: Overtopping conditions to which the levee at St. Philipsland was exposed, for $H_s = 2$m and T_m = 4.7s, and a storm duration of 2 hours

q $[l/s/m]$	0.1	1	10	30	50	75
P_{ot}	0.002	0.027	0.189	0.366	0.47	0.56
N_{ot}	3	42	289	561	720	858
V_p $[l/m]$	400	858	2110	3790	5180	6750

During the overtopping experiments at St. Philipsland initial damage spots were noticed around the respectively 4 and 7 m line below the crest line. At the 4 m line, which corresponds to $X = 3.7$ m, a minor bold spot was visible in the grass cover. At the 7 m line, which corresponds to $X = 6.5$ m, a minor headcut had formed. The initial damage spot around the 7 m line eventually developed into a big eroded area just above the toe.

The damage predictions for St. Philipsland experiment show two lines (See Figure 6). In the second graph the first line corresponds with $P_c = 22$ kN/m^2 which has been calibrated for the case whereby no damage occurred during the $1, 10,$ and 30 l/s per m test. The second line corresponds with $P_c = 33$ kN/m^2 which corresponds with the situation whereby no damage occurs during the $1, 10, 30,$ and 50 l/s per m tests. During the 30 l/s per m test some damage to the grass cover initiated at the connection with the boards bordering the side of the test section.

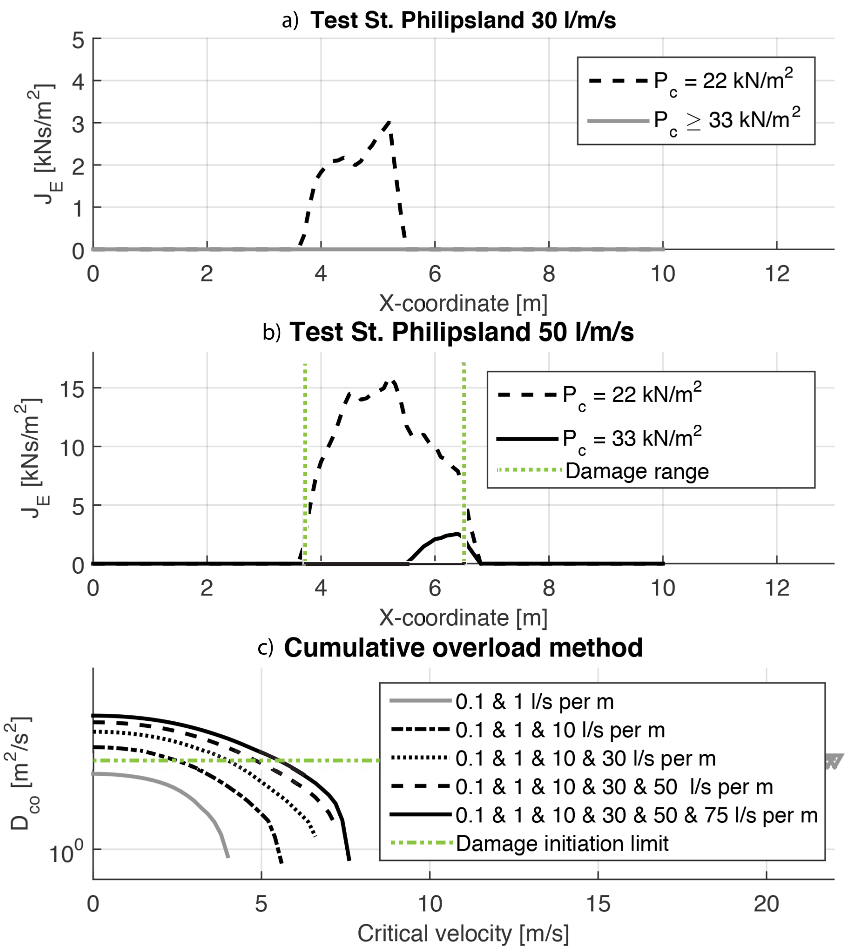

Figure 6: Distribution of excess momentum transferred to the landside slope if no failure occurred during for the 10 l/s per m experiment at St. Philipsland

During the 50 l/s per m test however the damage initiated on the test section itself at the 6m and 9 m distance from the outflow opening of the wave impact simulator. The slope started at 2 m distance from the outflow opening of the simulator. Hence, for a slope of $1 : 2.5$ the locations of the damage correspond with respectively $X = 3.7$m and $X = 6.5$m. These predictions are a close match with the actual location where damage initiated. The values of $P_c = 22$ kN$/$m^2 and $P_c = 33$ kN$/$m^2 correspond with values for the cohesion of $c' = 7.3$ kN$/$m^2 and $P_c = 11$ kN$/$m^2. Here the value of $P_c = 33$ kN$/$m^2 gives a better correspondance with the location of grass failure, and expected value for the cohesion.

4. Discussion

Evaluating the predictions of the wave impact approach has highlighted some interesting aspects. First the locations where the grass failures initiated were all subject to normal stresses indicating that a peak in momentum transfer may better describe the initiation of grass failure than a peak in stream power of the flow. At the test site at Wijmeers a clay layer was present at the landside slope which was protected by a poor quality grass cover. The grass cover failed during the first test at the location of a rabbit hole beneath the surface. The location of this rabbit hole is likely to have negatively influenced the resistance of the levee against overtopping. For a cohesive value of $4\ \mathrm{kN/m^2}$ however a good match is found between the peak excess momentum transfer and the location of damage during both the first and the second wave overtopping experiment. When applying the cumulative overload method to the Wijmeers experiment then one finds a critical velocity of 2 m/s. During the overflow experiments that were performed at Wijmeers it however became apparent that the grass cover was able to withstand flow velocities in excess of 3.5 m/s for up to 6 hours. The difference in flow velocity could be partially attributed to a difference in shear stress. However, in this case a critical stress may be a better parameter to use than a critical velocity value because stress could be directly related to the wave impact induced pressure. In some cases also an acceleration factor is applied to the cumulative overload method to account for the increase in velocity between the downstream end of the crest and the location where the damage occurred. In the case of Wijmeers however, damage initiated near the downstream end of the crest. It is therefore expected that the influence of the acceleration factor alone will not be able to explain the observed differences in critical velocity between the overtopping and overflow experiments. A clear difference between loading due to overflow and wave overtopping is that wave impacts induce significantly higher normal stresses on the levee at the point of reattachment than overflow. A normal stress based approach like the Wave Impact method is therefore able to explain why damage would occur during wave overtopping and not during overflow. The discrepancies found in the calibrated critical velocities and the resistance against the applied overflow velocities indicates that equations that apply a critical velocity parameter are not able to explain why a landside slope grass cover fails during wave overtopping but is able to withstand an overflow. The Wave Impact method is also able to indicate those locations along the landside slope where the highest wave overtopping induced load could be expected during a storm. The method indicates when damage is to be expected (i.e. $J_E > 0$ means damage) but it is limited in predicting the amount of damage caused by the overtopping waves, therefore, further research on the value of the magnitude of the excess momentum J_E is recommended. When a certain critical load indicator (for instance $J_{E,c}$) could be defined, indicating when the grass cover is classified as 'failed', the Wave Impact method predicts the wave overtopping induced landside slope damage more accurately.

For the St Philipsland case the wave impact method was able to accurately predict the location where damage would initiate after calibrating the critical pressure based on the tests during which no failure occurred. Due to the sole dependence of the damage coefficient in cumulative overload method on the critical velocity always one critical velocity value can be found for which the cumulative overload method accurately hind-casts at what moment damage initiated.

Estimates of the critical pressure were found to correspond well to the expected range of $P_c = 2 - 5c'$ whereby c' is the characteristic value for the undrained cohesion. It should be noted that for validation purposes the critical pressure and the critical velocity have been kept constant per dike section. The wave impact method thereby works with the assumption that the horizontal velocity of the wave does not change after it separates from the embankment. It is recommended to further study the validity of this assumption by measuring the location where the wave impacts on the landside slope. It is thereby recommended to also measure the impact pressures on the landside slope to identify whether these are significant enough to lead to failure of the grass cover. In the wave impact method the location of failure was related to the peak normal stresses that occurred. This hypothesis is strengthened by the observations of damage that occurred where the landside slope gradient of a levee reduces, for example due to a berm structure. In the cumulative overload method (Van der Meer et al., 2012) the shear stress is assumed to determine the moment of failure. It is recommended to further study which loading mechanism is dominant or whether grass failure is best described by a combination of these two loading mechanisms. For example, failure could be related to the total stress instead of just the normal stress component. The difference in the predicted critical velocities and the velocities obtained during the overflow tests during the Wijmeers experiments, and the high critical flow velocities does indicate occurrence of another initiation mechanism of the failure of the grass cover.

The authors acknowledge that also other effects influence the results of the existing models based on slope-parallel stresses. For instance, the turbulence intensities may vary along the slope leading to a change in (extreme) shear stresses, which is also not taken into account by these models. However, we do not believe that such an effect would explain the damage exactly at the location where the overtopping waves impact the slope.

5. Conclusions and Recommendations

This paper presents a new method for predicting the onset of failure of grass covered inner slopes of levees. The normal stresses exerted during wave overtopping events have been shown to exceed the resistance. The cumulative effect of normal stresses exerted by overtopping waves at the point of reattachment on the landside slope has been shown to be indicative of the onset of failure of grass covers. Besides the critical load at which damage to the grass cover commences, the method also predicts the location where damage will occur. The method has been validated against two wave overtopping field tests performed in The Netherlands and Belgium. However, the magnitude of the total excess momentum J_E at which the grass cover is classified as 'failed' is not jet defined. It is recommended to further study the critical magnitude of J_E and classify a critical load related to to condition of the grass cover. The new method was able to predict in 3 out of 4 cases the location where failure of the grass cover commenced. It is therefore recommended to further develop methods based on the peak transfer of momentum with the levee whereby the effects of normal stresses at the point of reattachment should be accounted for. In line with this further studies to the response of turf layers to momentum exchange by wave overtopping is recommended to improve the insights into the resistance of levees.

6. Bibliography

Bakker, J., Mom, R., Steendam, G., 2008. Factual report: Golfoverslagproeven zeeuwse dijken. Tech. rep., INFRAM, Marknesse, The Netherlands.

Cantré, S., Olschewski, J., Saathoff, F., 2017. Full-scale flume experiments to analyze the surface erosion resistance of dike embankments made of dredged materials. Journal of Waterway, Port, Coastal, Ocean Engineering 143 (3).

Dean, R., Rosati, J., Walton, T., Edge, B., Jan 2010. Erosional equivalences of levees: Steady and intermittent wave overtopping. Ocean Engineering 37, 104–113.

EurOtop, 2007. Wave Overtopping of Sea Defences and Related Structures: Assessment Manual.
URL `www.overtopping-manual.com`

Führböter, A., 1966. Der druckschlag durch brecher auf deichb´oschungen. Ph.D. thesis, Mitteilungen des Franzius-Instituts f´ur Grund- und Wasserbau der Technischen Universit´at Hannover.

Hai, T., Verhagen, H. J., 2014. Damage to grass covered slopes due to overtopping. In: ICCE 2014: Proceedings of 34th International Conference on Coastal Engineering, Seoul, Korea, 15-20 June 2014. Coastal Engineering Research Council.

Hewlett, H., 1985. Reinforcement of steep grassed waterways. Tech. Rep. 116, CIRIA, London.

Hoffmans, G., 2014. Wti 2017 onderzoek en ontwikkeling landelijk toetsinstrumentarium, product 5.8 validatie erosiebestendigheid. Tech. rep., Deltares.

Hughes, S., May 2011. Adaptation of the levee erosional equivalence method for the hurricane storm damage risk reduction system (hsdrrs). Tech. rep., US Army Core of Engineers, Engineer Research and Development Center.

Hughes, S. A., Thornton, C., Van der Meer, J., Scholl, B., 2012. Improvements in describing wave overtopping processes. In: Lynett, P., Smith, J. (Eds.), Coastal Engineering 2012. No. 33.

Miedema, S., 2014. The Delft Sand, Clay & Rock Cutting Model. IOS Press.

Richwien, W., 2003. Die widerstandsfähigkeit von deichen beim wellenüberlauf und die entwicklung von deichbrüchen-eine bestandsaufnahme.

Stanczak, G., 2007. Laboratory tests on the erosion of clay revetment of sea dike with and without a grass cover induced by breaking wave impact. Tech. rep., TU Braunschweig.

Stanczak, G., 2008. Breaching of sea dikes initiated from the seaside by breaking wave impacts. Ph.D. thesis.

van Damme, M., Ponsioen, L., Herrero, M., Peeters, P., 2016. Comparing overflow and wave-overtopping induced breach initiation mechanisms in an embankment breach experiment. In: E3S Web of Conferences. Vol. 7. EDP Sciences, p. 03004.

Van der Meer, J., van Hoven, A., Paulissen, A., Steendam, G., Verheij, H., Hoffmans, G., Kruse, G., 2012. Handreiking toetsen grasbekledingen op dijken t.b.v het opstellen van het beheerdersoordeel (bo) in de verlengde derde toetsronde. Tech. rep., Rijkswaterstaat, Ministerie van Infrastructuur en Milieu.

Van der Meer, W. J., 2002. Technisch rapport golfoploop en golfoverslag bij dijken, (dutch). Tech. rep.

Van der Schrieck, G., 2006. Dredging Technology CT5300.

Whitehead, E., Bull, W., Schiele, M., 1976. A guide to the use of grass in hydraulic engineering practice. Tech. rep.